The rapidity dependence of the proton-to-pion ratio in Au+Au and p+p collisions at $\sqrt{s_{NN}}$ = 62.4 GeV and 200 GeV

P. Staszel[a] for the BRAHMS collaboration

[a] *Smoluchowski Inst. of Physics, Jagiellonian University, ul. Reymonta 4, 30-059 Kraków, Poland*

Abstract

The BRAHMS measured proton-to-pion ratios in Au+Au and p+p collisions at $\sqrt{s_{NN}}$ = 62.4 GeV and $\sqrt{s_{NN}}$ = 200 GeV are presented as a function of transverse momentum and collision centrality within the pseudo-rapidity range $0 \leq \eta \leq 3.8$ The results for Au+Au at $\sqrt{s_{NN}}$ = 200 GeV are compared with predictions from models which incorporate hydro-dynamics, hadron rescattering and jet production, in the η interval covered. In Au+Au collisions at $\sqrt{s_{NN}}$ = 200 GeV, $\eta \approx 2.2$, and at $\sqrt{s_{NN}}$ = 62.4 GeV, $\eta = 0$, the bulk medium can be characterized by the common value of $\mu_B \approx 65$ MeV. The $p/\pi^+(p_T)$ ratios measured for these two selections display a striking agreement in the p_T range covered (up to 2.2 GeV/c). At collision energy of 62.4 GeV and forward pseudo-rapidity we found a crossing point of p/π^+ ratios measured in central and semi-peripheral Au+Au and in p+p reactions. The crossing occurs in the narrow η bin around value of 3.2, simultaneously in the whole covered p_T range (0.3 GeV/c $< p_T <$ 2 GeV/c).

The measured p_T dependence of the baryon-to-meson ratio appears to be related to modifications in the hadronization mechanisms as it happens in a partonic medium. It was pointed out that the baryon-to-meson ratio p_T dependence should be sensitive to the hadronization scenario due to the different quark content of baryons and mesons and/or to radial flow of the bulk medium because of significant differences in baryon and meson masses. Both flow and medium quark coalescence are expected to enhance protons over pions at intermediate p_T.

The PHENIX $\bar{p}/\pi^-$ data at mid-rapidity is well described by the Greco, Ko, and Levai quark coalescence model where the introduced coalescence involves partons from the medium (thermal) and partons from mini-jets [1]. The Hwa and Yang quark recombination model is also successful in describing BRAHMS and PHENIX mid-rapidity data for p/π^+ [2].

On the other hand, the comparison with the hydrodynamical model shows that hydro-flow cannot itself account for the large observed ratio above $\approx$ 3 GeV/c and that the model overpredicts the data at low p_T [3]. These results support the view of a hadronization process driven by parton recombination with negligible final state interactions between produced hadrons. Nevertheless, at large μ_B, a significant gap between the temperature of the transition from the partonic to the hadronic phase, T_c, and the temperature of chemical freeze-out is predicted by QCD lattice calculation. Thus at large μ_B, the picture, suggested by mid-rapidity measurements, might be contaminated by final state hadron interactions leading to a transition from the parton recombination scheme to a hydrodynamical description that has a common velocity field for baryons and mesons [4, 5].

The setup of the BRAHMS experiment is described in details in [6]. Here we just point

out that the arrangement of BRAHMS spectrometers, namely of the Mid-Rapidity Spectrometer (MRS) and the Forward Spectrometer (FS), makes it possible to measure identified particle spectra over a pseudo-rapidity interval from $\eta = 0$ to $\eta = 3.8$. Particle identification in the FS is provided by TOF measurements for low and medium particle momenta. High momentum particles are identified using a Ring Imaging Cherenkov detector (RICH) [7].

The data analysis utilizes the feature of the same pion and proton acceptance in the η versus p_T space in the same real time measurement. For a given η-p_T bin the p/π ratios are calculated on a setting by setting basis. In order to avoid mixing different PID techniques, which usually lead to different systematic uncertainties, the ratios are calculated separately for the TOF PID and the RICH PID. In this way all factors such as acceptance corrections, tracking efficiencies, trigger normalization and bias related to the centrality cut cancel out in the ratio. The only remaining corrections are those that are species related which are:

(i) decay in flight, interaction with the beam pipe and the detector material budget,
(ii) the PID efficiency correction.

The corrections for (i) are determined by the HIJING [8] simulations of heavy-ion collisions that are then feed as input to a realistic GEANT [9] model description of the BRAHMS experimental setup. We estimate that the overall systematic uncertainty related to this correction is at the level of 2%. The TOF PID is done separately for small momentum bins by fitting a multi-Gaussian function to the experimental squared mass M^2 distribution and applying a $\pm 3\sigma$ cut to select a given particle type. For measurements done with the FS spectrometer in the momentum range where pions overlap with kaons, (usually above 3.5 GeV/c) the RICH detector can be used in veto mode to select kaons with momentum smaller than the kaon Cherenkov threshold which is about 9 GeV/c. Above the proton threshold momentum which is about 15 GeV/c the RICH provides a direct proton identification. In this momentum range the RICH PID is based on the particle separation in the M^2 versus momentum space. The described PID procedure leads to a relatively clean sample of pions with some contamination by kaons having spurious rings associated in the RICH counter. Together with the kaon - proton overlap at larger momenta, this contamination effect is a source of systematic errors which have been estimated.

Figure 1 (left) shows p/π^+ ratios obtained for Au+Au reacting at $\sqrt{s_{NN}} = 200$ GeV for two centrality sets of events, namely, for centrality $0-10\%$ (solid dots) and $40-80\%$ (open squares) The shaded boxes plotted for the most central events only, represent the systematic uncertainties discussed in the previous section. The ratios extracted from p+p data at the same energy are plotted for comparison (solid stars). The p_T coverage depends on the pseudo-rapidity bins and extends up to $p_T = 4$ GeV/c for $\eta = 2.6$ and 3.1. At low p_T (< 1.5 GeV/c) the p/π^+ ratios exhibit a rising trend with a weak dependence on centrality. The dependency on centrality begins above 1.5 GeV/c. The ratios appear to reach a maximum value at p_T around 2.5 GeV/c (whenever there is enough p_T coverage). The maxima of the ratios increase with the level of centrality of the collision and at $\eta = 3.1$, are equal to about 2.5 and 1.5 for the $0-10\%$ and $40-80\%$ centrality bins, respectively. The p+p ratios are consistent with Au+Au data at low p_T and begin to deviate significantly above $p_T = 1$ GeV/c. At $\eta = 3.1$ a maximum value of the ratio of 0.55 is reached in p+p collisions which is a factor of 4.5 smaller than that observed for central Au+Au reactions.

The values of the $\bar{p}/\pi^-$ ratios plotted in Fig. 1 (right) are significantly lower than the p/π^+ ratios (note the difference in the vertical scale), however, the centrality dependence shows the same features as those observed in the p/π^+ ratios, namely, that the ratios for different centrality classes are consistent with each other up to $p_T \approx 1.2$ GeV/c and a strong dependence on centrality appears at larger transverse momenta reaching a maximum at similar p_T as the positive

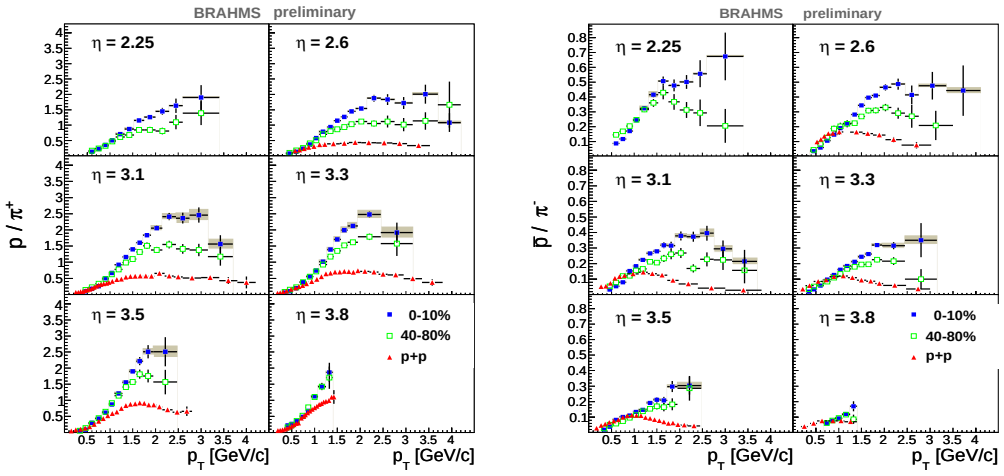

Figure 1: Centrality dependent p/π^+ (left) and $\bar{p}/\pi^-$ (right) ratio for Au+Au system colliding at $\sqrt{s_{NN}}$ = 200 GeV for central (0 – 10%) and semi-peripheral (40 – 80%) reactions in comparison with p+p collision data at the same energy. The vertical bars represent the statistical errors and the shaded boxes (plotted only for central Au+Au) show the systematic uncertainties.

particles. Looking at the p+p data alone, one can note the difference in shape between the p/π^+ and $\bar{p}/\pi^-$ ratios: a clear shift of the $\bar{p}/\pi^-$ peaks towards lower p_T , as well as a much broader p/π^+ peaks. These large difference between the Au+Au and p+p both in shape and overall magnitude may reflect significant medium effects in Au+Au at $\sqrt{s_{NN}}$ = 200 GeV in the pseudo-rapidity intervals covered.

Fig. 2 shows the p/π^+ ratios as function of p_T in the pseudo-rapidity range $2.6 < \eta < 3.8$ extracted from p+p reactions at $\sqrt{s}$ = 200 GeV. A very clear difference is found as the pseudo-rapidity changes from $\eta = 2.6$ to $\eta = 3.8$. But at high p_T all these ratios tend towards a common value of about 0.4 consistent with pQCD predictions [11]. Fig. 3 compares the p/π^+ ratio from p+p and Au+Au collisions at $\sqrt{s_{NN}}$ = 62.4 GeV and $\eta \approx 3.2$ ($\mu_B \approx 250$ MeV, [10]). There is remarkable little difference in the p/π^+ ratios over a very wide range of the colliding system volume, namely, from p+p reactions up to central Au+Au collisions. It should be note, that (what is now shown) at $\eta = 2.67$ the p/π^+ ratio from central Au+Au reactions is enhanced in respect to p+p collisions by a factor of 1.6, wheres at $\eta = 3.5$ the situation is reversed, namely, p/π^+ ratio in p+p exceeds that measured in central Au+Au by a factor of about 1.4. This indicates that the consistency observed at $\eta \approx 3.2$ is a results of simultaneous crossing of the ratios for differnt systems (from p+p up to central Au+Au) at this particular pseudorapidity bin.

We presented the (p_T) dependence of the p/π ratios measured in Au+Au and p+p collisions at energies 62.4 and 200 GeV as a function of pseudo-rapidity and collision centrality (Au+Au). The data provide the opportunity for studying baryon-to-meson production over a wide range of the baryo-chemical potential, μ_B. For Au+Au and p+p reactions at $\sqrt{s_{NN}}$ = 200 GeV the p/π^+ and $\bar{p}/\pi^-$ ratios show noticeable dependency on centrality at intermediate p_T with a rising trend from p+p to central Au+Au collisions. We have shown that p/π^+ ratios are remarkably similar for central Au+Au at $\sqrt{s_{NN}}$ = 200 GeV, $\eta \approx 2.2$ and central Au+Au at $\sqrt{s_{NN}}$ = 62.4 GeV, $\eta \approx 0$, where the bulk medium is characterized by the same value of $\bar{p}/p$ [12]. This observation, together with the observed centrality dependence suggests, that at these energies and pseudo-rapidity

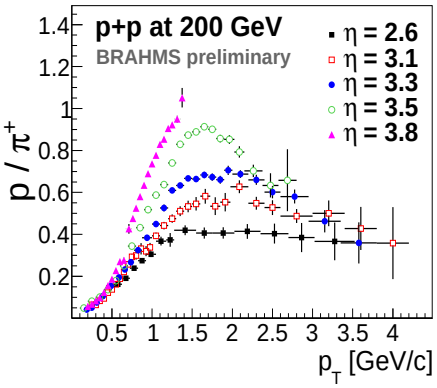

Figure 2: The p/π ratios at forward rapidities ($2.6 < \eta < 3.8$) in p+p at $\sqrt{s}$ = 200 GeV.

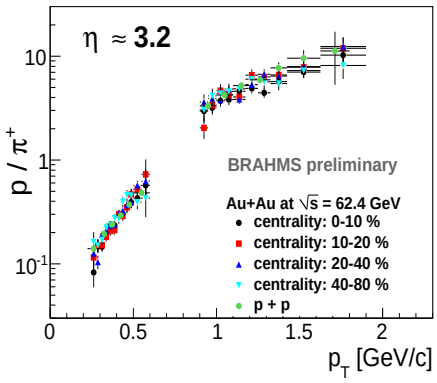

Figure 3: p/π^+ ratio from p+p and Au+Au collisions at $\sqrt{s_{NN}}$ = 62.4 GeV and $\eta \approx 3.2$.

intervals, particle production at intermediate p_T is governed by the size and chemical properties of the created medium. It was also shown that THERMINATOR, used as a reference model in our studies, underpredicts the p/π^+ and $\bar{p}/\pi^-$ ratios for central Au+Au at $\sqrt{s_{NN}}$ = 200 GeV at mid-rapidity. This is, however, expected within the picture of hadronization process driven by parton coalescence followed by weak final interactions of hadrons that can not bring different hadronic species to the common local collective velocity field assumed in the model. On the other hand THERMINATOR provides good quantitative description of data at forward rapidity, namely from $\eta \approx 2.2$ to ≈ 3.5. This may indicate that in this domain, the final hadronic interactions takes place long enough (before freeze-out) to suppress the relative collectivity of different species, which is a remnant effect of earlier hadronization via parton coalescence. Finally, the Au+Au and p+p measurements at $\sqrt{s_{NN}}$ = 62.4 GeV shows that the p/π^+ ratios for p+p and for all analysed Au+Au centralities cross simultaneously at the same η value (≈ 3.2) and are consistent with each other in the covered p_T range e.g. from 0.3 GeV/c up to 1.8 GeV/c.

References

[1] V. Greco, C.M. Ko, and P. Levai, Phys. Rev. Lett. **90** 022302 (2003).
[2] R. C. Hwa, and C. B. Yang, Phys. Rev. **C 67** 034902 (2003).
[3] E. J. Kim (BRAHMS Collaboration), Nucl. Phys. **A 774** 493-496 (2006).
[4] T. Hirano, and Y. Nara, Nucl. Phys. **A743** 305 (2004).
[5] W. Broniowski, and W. Florkowski, Phys. Rev. Lett. **87** 272302 (2001).
[6] M. Adamczyk et. al., BRAHMS Collaboration, Nucl. Instr. Meth. **A 499** 437 (2003).
[7] R. Debbe et. al., Nucl. Instr. Meth. **A 570** 216 (2007).
[8] M. Gyulassy and X. N. Wang, Comput. Phys. Commun. **83** 307 (1994).
[9] "GEANT: Detector Description and Simulation Tool", wwwinfo.cern.ch/asdoc/geant_html3/
[10] I.C. Arsene et. al., for BRAHMS Collaboration, Int. Jour. of Mod. Phys. **E 16** 2035 (2007).
[11] T. Hirano, and Y. Nara, Phys. Rev. **C 69**, 034908 (2004).
[12] F. Videbaek, Quark Matter 2009, this proceedings.